Light: Science & Applications (2017) 6, e16254; doi:10.1038/lsa.2016.254
Official journal of the CIOMP 2047-7538/17
www.nature.com/lsa

ORIGINAL ARTICLE

Reconfigurable metasurfaces that enable light polarization control by light

Meng-Xin Ren[1,2], Wei Wu[1], Wei Cai[1], Biao Pi[1], Xin-Zheng Zhang[1] and Jing-Jun Xu[1]

Plasmonic metasurfaces have recently attracted much attention because of their novel characteristics with respect to light polarization and wave front control on deep-subwavelength scales. The development of metasurfaces with reconfigurable optical responses is opening new opportunities in high-capacity communications, real-time holograms and adaptive optics. Such tunable devices have been developed in the mid-infrared spectral range and operated in light intensity modulation schemes. Here we present a novel optically reconfigurable hybrid metasurface that enables polarization tuning at optical frequencies. The functionality of tuning is realized by switching the coupling conditions between the plasmonic modes and the binary isomeric states of an ethyl red switching layer upon light stimulation. We achieved more than 20° nonlinear changes in the transmitted polarization azimuth using just 4 mW of switching light power. Such design schemes and principles could be easily applied to dynamically adjust the functionalities of other metasurfaces.
Light: Science & Applications (2017) **6,** e16254; doi:10.1038/lsa.2016.254; published online 2 June 2017

Keywords: azo ethyl red; metasurfaces; nonlinear polarization modulation; photoisomerization; reconfigurable

INTRODUCTION

Metasurfaces, as two-dimensional equivalents of metamaterials, are ultrathin optical components consisting of artificially designed arrays of meta-atoms. Metasurfaces can impart control over the phase, polarization and local wave front of light at deep-subwavelength scales[1,2]. A plethora of progress has already been achieved in the development of metasurfaces, such as interfaces showing anomalous refraction or reflection[3–5], the generation of vortex beams[6,7], ultrathin metalenses[8–10], novel quarter-wave plates[11,12], the optical spin-Hall effect[13,14], continuous harmonic nonlinearity phase control[15] and high resolution holograms[16–19]. However, most of the reported metasurfaces are passive, that is, the functionalities are predefined after the fabrication process and cannot be reconfigured dynamically. Substantial efforts are now dedicated to exploring metasurfaces with tunable responses; such metasurfaces would enable unprecedented applications, such as high-capacity communications, dynamic beam shaping and real-time holograms. To date, a number of techniques for such tunable components have emerged based on thermal[20], mechanical[21,22], optical[23] and electrical mechanisms[24–26]. Nevertheless, above tunable metasurfaces are conventionally operated in the mid-infrared and THz spectral range and are based on light intensity modulation. Here we experimentally demonstrate a reconfigurable metasurface at optical wavelengths that exhibits tunable polarization behavior upon light stimulation. In our paradigm, we combine the metallic nanostructure layer with a switching layer, that is, a thin layer of photoisomerizable azo ethyl red, where the coupling between the resonant plasmonic modes and the switchable isomeric states of ethyl-red polymer leads to more than 20° nonlinear optical polarization modulation under weak continuous wave (CW) switching laser excitation of just a few milliwatts. Such components open the gateway toward the creation of various photonic functions, including dynamic spatial light modulation, pulse shaping, subwavelength imaging or sensing, novel quantum optics devices and real-time holograms.

MATERIALS AND METHODS

The metasurface consists of a periodic array of L-shaped slits, each of which were cut via focused ion-beam milling through a 100-nm-thick gold film supported by a 500-μm-thick fused quartz substrate (as shown in Figure 1a). The period of the metasurface lattice is 300 nm, with an entire array footprint of $50 \times 50\ \mu m^2$. To combine the metasurface with the switching layer, ethyl-red powder (TCI, Tokyo, Japan) was first dissolved in ethanol to produce a solution with a concentration of ~18 wt-%. Next, the solution was mixed with polymethylmethacrylate (PMMA, Allresist GmbH, Strausberg, Germany) at a volume ratio (v/v) of 50%. The resulting polymer mixture was spin coated onto the metasurface (1500 rpm), forming an ~300-nm-thick layer. To investigate the polarization effects of the metasurface, a polarimeter consisting of a rotating super-achromatic quarter-wave plate and a Glan–Taylor calcite polarizer was used (see Supplementary Information)[27,28]. In our experiment, the light beam was normally incident and polarized along the *x* direction; in this case, ~30% of the light is transmitted through the sample (see Figure 1b, measured using a commercial microspectrophotometer (IdeaOptics Technologies, Shanghai, China)).

[1]The Key Laboratory of Weak-Light Nonlinear Photonics, Ministry of Education, School of Physics and TEDA Institute of Applied Physics, Nankai University, Tianjin 300071, China and [2]The 2011 Project Collaborative Innovation Center for Biological Therapy, Nankai University, Tianjin 300071, China
Correspondence: JJ Xu, Email: jjxu@nankai.edu.cn; MX Ren, Email: ren_mengxin@nankai.edu.cn
Received 22 August 2016; revised 10 November 2016; accepted 10 November 2016; accepted article preview online 16 November 2016

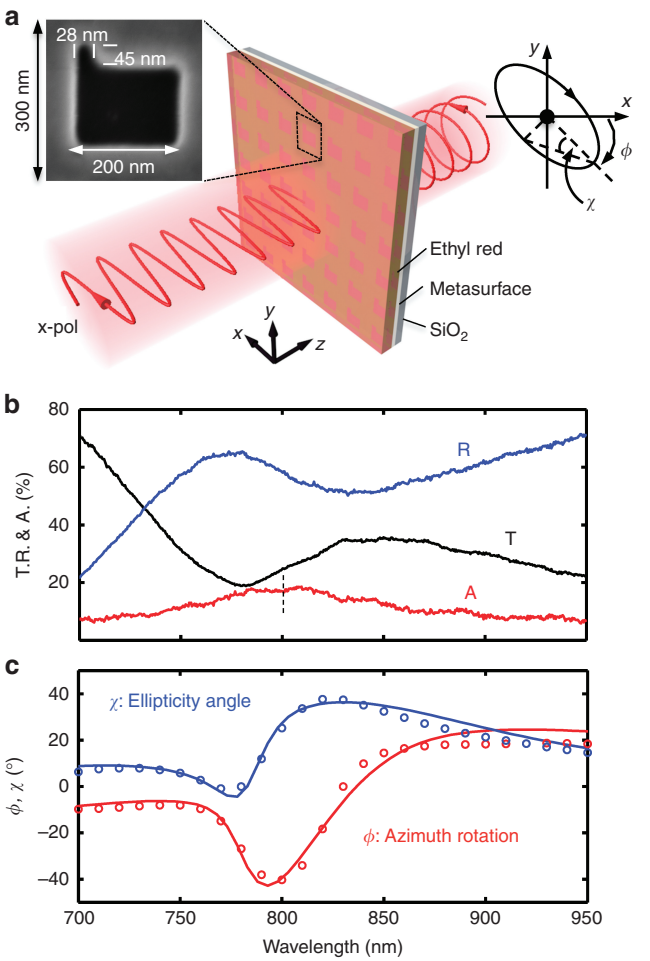

Figure 1 Polarization effects of the plasmonic nanostructure. (**a**) Because the metasurface is chiral and anisotropic in structure, a linearly polarized wave becomes elliptically polarized and its polarization azimuth rotates after passing through the nanostructure. Changes in the polarization states in the transmitted wave compared with the incident wave are defined by polarization azimuth rotation ϕ and ellipticity angle χ. Positive values of ϕ and χ correspond to the clockwise rotation of the polarization azimuth and a right-handed polarization ellipse, respectively, as observed against the propagation direction. The scanning electron micrograph shows a single meta-atom along with the dimensions. (**b**) The spectra of the hybrid metasurface. T corresponds to transmission; R corresponds to reflection; and A corresponds to absorption. (**c**) Spectral dependence of the polarization changes by the nanostructure in terms of polarization azimuth rotation ϕ and ellipticity angle χ in the wavelength range of 700–950 nm (circles show the experimental data points, solid curves are simulation results).

RESULTS AND DISCUSSION

The individual meta-atoms are chiral and anisotropic in geometry. Thus, a wave with initially linear polarization would become elliptically polarized, and its polarization azimuth rotates after passing through such a medium (as illustrated in Figure 1a)[29,30]. The polarization modifications to the incident light are characterized in terms of polarization azimuth rotation ϕ and ellipticity angle χ in the wavelength range of 700–950 nm, as shown in Figure 1c. We achieved an azimuth angle rotation ϕ as high as 40° (red in Figure 1c) at 800 nm from the nanostructures, whose negative sign corresponds to the counter-clockwise rotation direction of the polarization azimuth as viewed by an observer looking into the beam. However, at the longer wavelengths, ϕ reverses to be positive and the azimuth rotates in the clockwise direction. In addition, the ellipticity angle χ (shown in blue) reaches ~37° at 820 nm. Moreover, its positive signs in the studied wavelength range indicate the right-handed polarized feature of the transmitted light (the end of the electric field vector rotates clockwise around the polarization ellipse, as observed against the propagation direction, see Supplementary Information for more information about polarization). Our measured results (circles in Figure 1c) could be well explained by the numerical simulations (solid curves in Figure 1c, and see Supplementary Information for more simulation details). Note that the metasurface exhibits a plasmonic absorption resonance at ~800 nm, where the azimuth rotation is also largest. This result implies the underlying relationship between the polarization effects and plasmonic resonances in our structure.

The tuning over the polarization effects relies on the modulation of the coupling situations between the plasmonic modes and the isomeric ethyl-red polymers. In our experiment, this tuning is achieved by irradiating the nanostructure by green light (532 nm, *y*-polarized, generated from a semiconductor pumped solid-state CW laser). It is well known that the changes in the dielectric properties of ambient media could efficiently modify the plasmonic response of the coupled metallic nanostructures[31,32]. In our configurations, under external optical stimuli, the photoactive azo molecule structures effectively convert from the trans state to the cis state (Figure 2b). In addition, when the green light is blocked, the ethyl-red molecules return to its trans state through thermal relaxation in the dark. Such structural modifications result in changes of the molecular polarizability and finally change the refractive index of the polymer layer according to the Lorentz–Lorenz-condition[33,34]. Hence, the plasmonic resonance and the resulting polarization effects of the hybrid metasurfaces are optically switched. In the experiment, the green light was 4 mW in power and was focused to a spot size of 9 μm in diameter, corresponding to an intensity of ~ 6.3 kW cm^{-2}, which is sufficient to observe large nonlinear modifications to the transmitted signal light polarization states without damaging the device (the damage threshold was measured to be ~9.5 kW cm^{-2}). As illustrated by Figure 2c, the most obvious effects of introducing control light are the dramatic blue shifts in the ϕ and χ curves corresponding to optically induced decreases in refractive index for cis-ethyl-red[33] (see Supplementary Information for simulation details). Because the refractive index change of the polymer layer is determined by the number of molecules that undergo structural modification, the polarization modulation magnitudes is adjustable by changing the power of the control light. The optically induced nonlinear changes in the polarization parameters ($\Delta\chi$ and $\Delta\phi$) for various green light power levels are shown in Figure 2d. The $\Delta\chi$ curves were found to exhibit pronounced peaks between 760 and 820 nm, implying an increase in transmitted ellipticity angle for increased control light intensity. However, the $\Delta\phi$ curves exhibit peaks between 790 and 840 nm, leading to the smaller total azimuth rotation as the control light intensity increases. The $\Delta\chi$ and $\Delta\phi$ at 790 and 820 nm, respectively, as a function of green light power are given in Figure 2e. $\Delta\chi$ and $\Delta\phi$ achieve values of ~16.7° and 23.2°, respectively, for 4 mW of green light excitation. These numbers are more than one order-of-magnitude larger than the previously reported nonlinear extrinsic optical activity effects from split-ring metamaterials (only ~1° nonlinear polarization changes under ~1 GW cm^{-2} excitation)[35]. More importantly, rather than the self-nonlinear polarization action of one single beam[35], the device shown here demonstrates inter-beam polarization control by one beam over another, which is technically essential for realizing all-optical modulator or switching. Furthermore, in this case, the control

doi:10.1038/lsa.2016.254

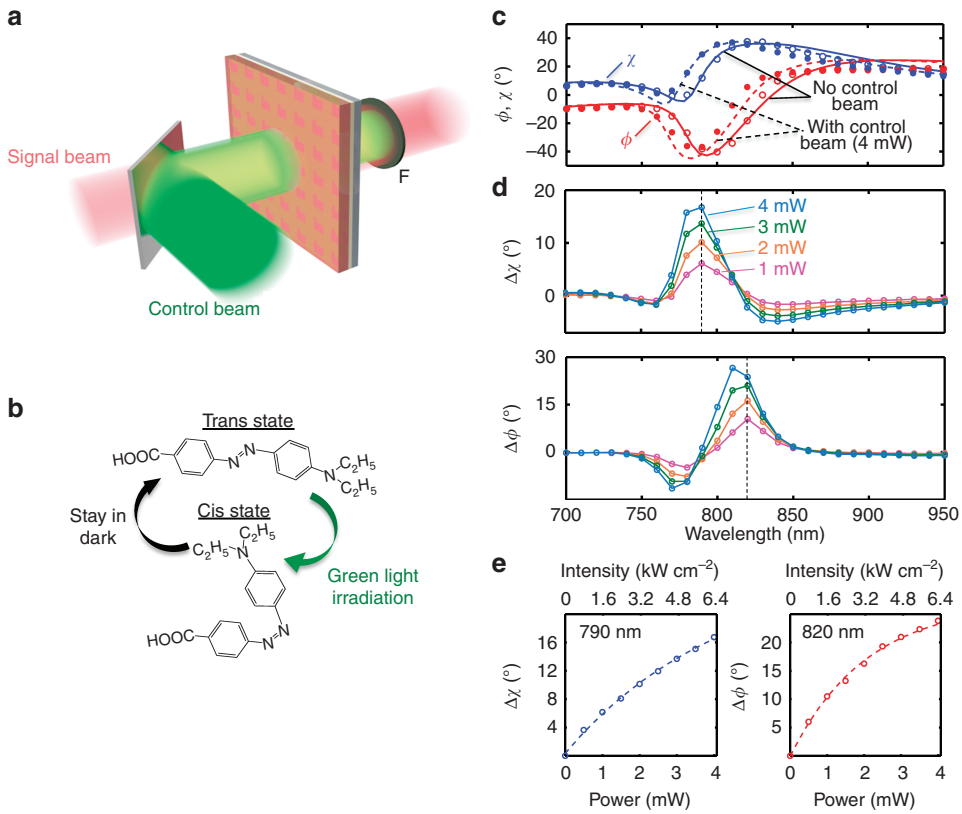

Figure 2 Nonlinear tuning over polarization effects of the plasmonic metasurfaces. (**a**) Green light (532 nm) is used as a control beam to switch the polarization effects of the nanostructure. The signal and control beams were combined together by a dichroic mirror. A long pass filter (F) with cut-on wavelength at 550 nm was applied to isolate the green light in the transmitted light. (**b**) Under irradiation of green light, each ethyl-red molecule isomerizes from the trans state to the cis state and then recovers to the original trans state through thermally relaxation in dark. (**c**) Under green light (4 mW) excitation, both ϕ and χ (solid dots: measured data, dashed lines: simulation results) undergo an obvious blue shift compared with the results without the control beam (circles: measured data, solid lines: simulation results). (**d**) Measured nonlinear changes in the polarization parameters for various control light powers relative to results without the control beam. Vertical dashed lines indicate the wavelengths at which the power dependences of $\Delta\phi$ and $\Delta\chi$ are shown in (**e**).

light could be from a low-power CW laser rather than an ultrashort laser pulse. These features would make the device much more convenient to implement in real applications.

To characterize the temporal properties of the tunable polarization effects, the green light (4 mW) was mechanically chopped, thereby causing dynamic refractive index changes in the polymer layer and resulting in dynamic modulations over the signal light. The signal light was chosen at 820 nm, where the nonlinear change of azimuth rotation is large. To achieve the rise/fall edge that is as short as possible in the modulated control light (measured as <12 μs between 10% and 90% amplitudes), the chopper blade was placed near a focal point of the green beam. The quarter-wave plate and Glan–Taylor prism were properly orientated to obtain extinction of the transmitted signal light initially. Thus, any modulations in polarization states were converted into the modulations of light intensity that leaked from the polarimeter and were monitored by the oscilloscope. In this manner, we technically built an intensity modulator based on our tunable metasurface that can be used in an optical display or a data encoder in a telecommunication system. Figure 3 shows the dynamic response of the signal light under different modulating frequencies. The horizontal dashed lines show the background level of the signal before green light excitation. Under excitation of the control light, the output signals increased from a very low level to a stable level. Next, when the chopper blade obstructed the control beam, the output signals started to decay. The modulation depth reaches ~80% at 6 Hz. Using the biexponential fitting[36], the rise and decay rates of fast (and slow) components are ~0.8 (and 14.7) and 0.3 (and 40.2) ms, respectively. For higher modulation frequency, the modulation depth decreases gradually, reducing to ~53% and 25% at 25 and 100 Hz, respectively. Considering the transmission of the signal light is a transient process, the ultimate speed of our polarization modulation is limited by both the isomerization and structural recovery times of the polymer. Such processes are not 'fast' switches compared with the commercial electro-optical modulations (normally on the level of several nanoseconds). However, the response time could be further reduced by using a dual-beam pump scheme[37] or by replacing the switching layer with materials of faster nonlinear responses, such as semiconducting materials[38,39] or chalcogenide phase-change media[40].

It may be expected that the operating wavelength range of our hybrid plasmonic polarization modulation frameworks could be flexibly tuned by simple adjustment of geometric dimensions of the metasurface. By shifting the spectral range to shorter wavelengths for RGB primary colors, the metasurface will be very useful in novel all-optical display devices. Moreover, by tuning the signal light wavelength to the telecommunications wavelength band, such devices could function as data encoders for interconnecting visible light communication systems and fiber telecommunication systems without any optoelectronic conversions. Note that for thin ethyl-red polymer films,

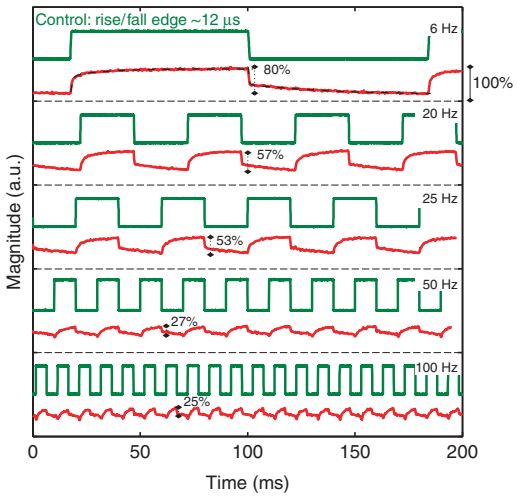

Figure 3 Speed characterization of the nonlinear polarization effect. Dynamic response of the nonlinear polarization effects under green light modulations. The chopped green light (shown by green curves) acts as the trigger reference for an oscilloscope. The red curves show the temporal response of the transmitted signal light, along with the double-exponential fitting curves. The horizontal dashed lines present the background level of the signal light before green light excitation.

their optical performances could be degraded by phase separation and micro-crystallization inside the film[41] or surface contamination caused by dust in air. An extra protection layer or covalent bonding of the azo moiety to the host polymer matrix[41] could extend the lifetime of the whole device; a longer lifetime is useful in real applications.

CONCLUSION

In conclusion, we demonstrated a novel platform for creating dynamically reconfigurable optical devices that can achieve all-optical polarization control under weak optical excitation at optical frequencies. Our results could lead to breakthroughs in applications such as highly compact polarization (or intensity) modulating elements for optical computing/communications, novel optical display devices and encoders for quantum information processing by eliminating optoelectronic conversions and markedly reducing the size of the polarization modulation architectures. Furthermore, such modulation principles and schemes could be extended and applied to tune other metasurface functionalities, thereby creating various photonic functions such as dynamic spatial light modulation, pulse shaping, subwavelength imaging or sensing, novel quantum optics and real-time holograms.

CONFLICT OF INTEREST

The authors declare no conflict of interest.

ACKNOWLEDGEMENTS

We acknowledge the support from the National Basic Research Program of China (2013CB328702, 2010CB934101), the National Natural Science Foundation of China (11304162, 11374006), the 111 Project (B07013), PCSIRT (IRT_13R29), SRFDP (20130031120005), the Fundamental Research Funds for the Central Universities and the Collaborative Innovation Center of Extreme Optics.

1 Meinzer N, Barnes WL, Hooper IR. Plasmonic meta-atoms and metasurfaces. *Nat Photonics* 2014; **8**: 889–898.
2 Yu NF, Capasso F. Flat optics with designer metasurfaces. *Nat Mater* 2014; **13**: 139–150.
3 Ni XJ, Emani NK, Kildishev AV, Boltasseva A, Shalaev VM. Broadband light bending with plasmonic nanoantennas. *Science* 2012; **335**: 427.
4 Huang LL, Chen XZ, Mühlenbernd H, Li GX, Bai BF *et al.* Dispersionless phase discontinuities for controlling light propagation. *Nano Lett* 2012; **12**: 5750–5755.
5 Sun SL, Yang KY, Wang CM, Juan TK, Chen WT *et al.* High-efficiency broadband anomalous reflection by gradient meta-surfaces. *Nano Lett* 2012; **12**: 6223–6229.
6 Yu NF, Genevet P, Kats MA, Aieta F, Tetienne JP *et al.* Light propagation with phase discontinuities: generalized laws of reflection and refraction. *Science* 2011; **334**: 333–337.
7 Yang YM, Wang WY, Moitra P, Kravchenko II, Briggs DP *et al.* Dielectric meta-reflectarray for broadband linear polarization conversion and optical vortex generation. *Nano Lett* 2014; **14**: 1394–1399.
8 Aieta F, Genevet P, Kats MA, Yu NF, Blanchard R *et al.* Aberration-free ultrathin flat lenses and axicons at telecom wavelengths based on plasmonic metasurfaces. *Nano Lett* 2012; **12**: 4932–4936.
9 Pors A, Nielsen MG, Eriksen RL, Bozhevolnyi SI. Broadband focusing flat mirrors based on plasmonic gradient metasurfaces. *Nano Lett* 2013; **13**: 829–834.
10 Aieta F, Kats MA, Genevet P, Capasso F. Multiwavelength achromatic metasurfaces by dispersive phase compensation. *Science* 2015; **347**: 1342–1345.
11 Yu NF, Aieta F, Genevet P, Kats MA, Gaburro Z *et al.* A broadband, background-free quarter-wave plate based on plasmonic metasurfaces. *Nano Lett* 2012; **12**: 6328–6333.
12 Zhao Y, Alù A. Tailoring the dispersion of plasmonic nanorods to realize broadband optical meta-waveplates. *Nano Lett* 2013; **13**: 1086–1091.
13 Li GX, Kang M, Chen SM, Zhang S, Pun EYB *et al.* Spin-enabled plasmonic metasurfaces for manipulating orbital angular momentum of light. *Nano Lett* 2013; **13**: 4148–4151.
14 Yin XB, Ye ZL, Rho J, Wang Y, Zhang X. Photonic spin hall effect at metasurfaces. *Science* 2013; **339**: 1405–1407.
15 Li GX, Chen SM, Pholchai N, Reineke B, Wong PWH *et al.* Continuous control of the nonlinearity phase for harmonic generations. *Nat Mater* 2015; **14**: 607–612.
16 Walther B, Helgert C, Rockstuhl C, Setzpfandt F, Eilenberger F *et al.* Spatial and spectral light shaping with metamaterials. *Adv Mater* 2012; **24**: 6300–6304.
17 Ni XJ, Kildishev AV, Shalaev VM. Metasurface holograms for visible light. *Nat Commun* 2013; **4**: 2807.
18 Chen WT, Yang KY, Wang CM, Huang YM, Sun G *et al.* High-efficiency broadband meta-hologram with polarization-controlled dual images. *Nano Lett* 2014; **14**: 225–230.
19 Zheng GX, Mühlenbernd H, Kenney M, Li GX, Zentgraf T *et al.* Metasurface holograms reaching 80% efficiency. *Nat Nanotechnol* 2015; **10**: 308–312.
20 Rensberg J, Zhang SY, Zhou Y, McLeod AS, Schwarz C *et al.* Active optical metasurfaces based on defect-engineered phase-transition materials. *Nano Lett* 2016; **16**: 1050–1055.
21 Gutruf P, Zou CJ, Withayachumnankul W, Bhaskaran M, Sriram S *et al.* Mechanically tunable dielectric resonator metasurfaces at visible frequencies. *ACS Nano* 2016; **10**: 133–141.
22 Ee HS, Agarwal R. Tunable metasurface and flat optical zoom lens on a stretchable substrate. *Nano Lett* 2016; **16**: 2818–2823.
23 Wang Q, Rogers ETF, Gholipour B, Wang CM, Yuan GH *et al.* Optically reconfigurable metasurfaces and photonic devices based on phase change materials. *Nat Photonics* 2016; **10**: 60–65.
24 Yao Y, Kats MA, Shankar R, Song Y, Kong J *et al.* Wide wavelength tuning of optical antennas on graphene with nanosecond response time. *Nano Lett* 2014; **14**: 214–219.
25 Yao Y, Shankar R, Kats MA, Song Y, Kong J *et al.* Electrically tunable metasurface perfect absorbers for ultrathin mid-infrared optical modulators. *Nano Lett* 2014; **14**: 6526–6532.
26 Miao ZQ, Wu Q, Li X, He Q, Ding K *et al.* Widely tunable terahertz phase modulation with gate-controlled graphene metasurfaces. *Phys Rev X* 2015; **5**: 041027.
27 Bass M, DeCusatis C, Enoch J, Lakshminarayanan V, Li GF *et al. Handbook of Optics, Third Edition Volume I: Geometrical and Physical Optics, Polarized Light, Components and Instruments(set)*, 3rd edn. New York: McGrawHill, Inc.; 2010.
28 Ren MX, Chen M, Wu W, Zhang LH, Liu JK *et al.* Linearly polarized light emission from quantum dots with plasmonic nanoantenna arrays. *Nano Lett* 2015; **15**: 2951–2957.
29 Canfield BK, Kujala S, Kauranen M, Jefimovs K, Vallius T *et al.* Remarkable polarization sensitivity of gold nanoparticle arrays. *Appl Phys Lett* 2005; **86**: 183109.
30 Plum E, Fedotov VA, Zheludev NI. Asymmetric transmission: a generic property of two-dimensional periodic patterns. *J Opt* 2010; **13**: 024006.
31 Homola J. Surface plasmon resonance sensors for detection of chemical and biological species. *Chem Rev* 2008; **108**: 462–493.
32 Ren MX, Pan CP, Li QQ, Cai W, Zhang XZ *et al.* Isotropic spiral plasmonic metamaterial for sensing large refractive index change. *Opt Lett* 2013; **38**: 3133–3136.
33 Lückemeyer T, Franke H. Nonlinear and bistable properties of doped pmma lightguides. *Appl Phys A* 1992; **55**: 41–48.
34 Kittel C. *Introduction to Solid State Physics*, 8th edn. New York: Wiley; 2005.
35 Ren MX, Plum E, Xu JJ, Zheludev NI. Giant nonlinear optical activity in a plasmonic metamaterial. *Nat Commun* 2012; **3**: 833.
36 Such G, Evans RA, Yee LH, Davis TP. Factors influencing photochromism of spiro-compounds within polymeric matrices. *J Macromol Sci C* 2003; **43**: 547–579.

37 Lu WQ, Chen GY, Hao ZF, Xu JJ, Tian JG *et al*. Enhancement of modulation depth of an all-optical switch using an azo dye-ethyl red film. *Chin Phys B* 2010; **19**: 084208.
38 Dani KM, Ku Z, Upadhya PC, Prasankumar RP, Brueck SRJ *et al*. Subpicosecond optical switching with a negative index metamaterial. *Nano Lett* 2009; **9**: 3565–3569.
39 Cho DJ, Wu W, Ponizovskaya E, Chaturvedi P, Bratkovsky AM *et al*. Ultrafast modulation of optical metamaterials. *Opt Express* 2009; **17**: 17652–17657.
40 Ríos C, Stegmaier M, Hosseini P, Wang D, Scherer T *et al*. Integrated all-photonic non-volatile multi-level memory. *Nat Photonics* 2015; **9**: 725–732.
41 Shahinpoor M, Schneider HJ. *Intelligent Materials*. Cambridge: Royal Society of Chemistry; 2008.

This work is licensed under a Creative Commons Attribution-NonCommercial-ShareAlike 4.0 International License. The images or other third party material in this article are included in the article's Creative Commons license, unless indicated otherwise in the credit line; if the material is not included under the Creative Commons license, users will need to obtain permission from the license holder to reproduce the material. To view a copy of this license, visit http://creativecommons.org/licenses/by-nc-sa/4.0/

© The Author(s) 2017

Supplementary Information for this article can be found on the *Light: Science & Applications*' website (http://www.nature.com/lsa).